HHS Public Access

Author manuscript

Int J Radiat Biol. Author manuscript; available in PMC 2022 September 06.

Published in final edited form as:

Int J Radiat Biol. 2022 ; 98(5): 913–923. doi:10.1080/09553002.2021.1998708.

Pseudo Pelger-Huët anomalies as potential biomarkers for acute exposure radiation dose in rhesus macaques *(Macaca mulatta)*

Joshua M. Hayes[a,b], **John D. Olson**[c], **Yuiko Chino**[a], **J. Daniel Bourland**[d], **J. Mark Cline**[c], **Thomas E. Johnson**[a]

[a]Department of Environmental and Radiological Health Sciences, Colorado State University, Fort Collins, Colorado, USA

[b]Biological Dosimetry Model Laboratory, Section of Applied Radiation Biology and Radiotherapy, Division of Human Health, Department of Nuclear Sciences and Applications, International Atomic Energy Agency, Vienna, Austria

[c]Wake Forest School of Medicine, Department of Pathology, Section on Comparative Medicine, Winston-Salem, NC, USA

[d]Wake Forest School of Medicine, Department of Radiation Oncology, Winston-Salem, NC, USA

Abstract

Purpose: The potential for malicious use of radiation, or radiation accidents could potentially lead to acute, high radiation doses to the public. Following acute accidental exposure to high doses of radiation, medical intervention is pivotal to the survivability of the patient, and the sooner the appropriate measures are taken the better the odds for survival. Early estimates of acute accidental radiation doses can be determined via biomarkers such as dicentric chromosome analysis or scenario reconstruction using computer software. However, both take valuable time and can be expensive. Increased frequencies of abnormal neutrophils in peripheral blood, referred to as pseudo Pelger-Huët anomalies (PPHAs), have been shown to be potential biomarkers of radiation

CONTACT Joshua M. Hayes jmhayes612@gmail.com Biological Dosimetry Model Laboratory, Section of Applied Radiation Biology and Radiotherapy, Division of Human Health, Department of Nuclear Sciences and Applications, International Atomic Energy Agency, Vienna, Austria.

Notes on contributors

Joshua M. Hayes, Ph.D., is an Associate Radiobiologist/Biodosimetrist at the Biological Dosimetry Model Laboratory, in the section of Applied Radiobiology and Radiotherapy, Division of Human Health, Department of Nuclear Sciences and Applications, International Atomic Energy Agency, Vienna, Austria.

John D. Olson, MS, MS, is a Research Associate and Resource Manager for the NHP Radiation Late Effects Cohort at the Department of Pathology Section on Comparative Medicine, School of Medicine, Wake Forest University, Winston-Salem, NC, USA.

Yuiko Chino, MS, is a Ph.D. Candidate in the Department of Environmental and Radiological Health Sciences, Colorado State University, Fort Collins, Colorado, USA, 80523-1618.

J. Daniel Bourland, Ph.D., is Professor, Departments of Radiation Oncology, Physics, and Biomedical Engineering a Department of Radiation Oncology Wake Forest School of Medicine, Wake Forest University, Winston-Salem, NC, USA.

J. Mark Cline, DVM, Ph.D., DACVP, is a Professor of Pathology/Comparative Medicine and Radiation Oncology at Wake Forest School of Medicine, Winston-Salem, NC, USA.

Thomas E. Johnson, Ph.D., is a Professor in the Department of Environmental and Radiological Health Sciences Colorado State University, Fort Collins, CO, USA.

Disclosure statement

The authors declare no actual or potential conflict of interest including any financial, personal, or other relationships with other persons or organizations that could inappropriately influence their work. The authors alone are responsible for the content and writing of this paper.

Supplemental data for this article can be accessed here.

exposure in several scenarios, including the 1958 Y-12 criticality accident and the radium dial painters. PPHAs are potentially a faster and cheaper quantitative biomarker for radiation exposure, and here they were evaluated in acutely exposed rhesus macaques.

Methods and materials: Peripheral blood smears from acutely exposed rhesus macaques were evaluated for the percentage of neutrophils that displayed the PPHA morphology using light microscopy. Irradiated animals received 0 to 8.5 Gy total body radiation using one of two strategies: (1) linear accelerator-produced 6 MV photons delivered at 80 cGy/minute; or (2) Cobalt 60-produced gamma irradiation delivered at 60 cGy/min. Zero dose animals were used to determine a baseline percentage of PPHAs, and blood smears taken periodically throughout the lifetime of exposed animals post-irradiation were used to determine the persistence and biokinetics of PPHAs.

Results: The baseline prevalence of the PPHA in rhesus macaques was determined to be 0.58 ± 0.46%. The dose-response curve with doses ranging from 0 Gy to 8.5 Gy (LD90/30) displayed a strong positive correlation between PPHA percentage and acute radiation dose (R^2 of 0.88 $p = 3.62 \times 10^{-22}$). Statistically significant differences were found when animals were separated into dose cohorts of 0, 4, 6.4–6.5, and 8–8.5 Gy. The biokinetics model utilized only 4 Gy exposures and blood smears taken periodically over 3.1 years post-irradiation. PPHA morphology increases quickly following irradiation and appears stable over 3.1 years post-irradiation.

Conclusion: PPHA morphology was confirmed to be present in rhesus macaques, a dose-response relationship was constructed, and it is stable over 3 years post-irradiation. This study demonstrates that PPHA analysis can be a fast and cheap method of biodosimetry. Future studies will work to determine the accuracy of dose determination and lower limits of detection.

Keywords

Biodosimetry; biomarkers; pseudo Pelger-Huët anomaly; rhesus macaque; dose-response curve

Introduction

Radiation exposure can occur in several different ways to include but not limited to internal, external, chronic, acute, industrial accidents, environmental contamination, naturally occurring radioactive materials, criticality accidents, or combinations of the above. Considering the multiple scenarios for accidental radiation exposures that have happened and could happen, tools for early dose assessments are vital to proper triage of patients and ultimately medical treatment. The PPHA is proposed as an expansion upon the methodologies available to biodosimetrists for early and retrospective dose estimations for individuals that have been exposed to ionizing radiation.

Biodosimetry is the science of using a biological, physiological, or chemical marker for the purposes of reconstructing a dose of ionizing radiation (Sullivan et al. 2013). While there are many techniques in use today, the immense variety of scenarios in which people can be exposed renders no one assay as the best method, let alone a standalone assay. Many factors include detection limits, number of patients, other hazards to life and well-being of both patients and the caregivers, accessibility to necessary laboratory equipment, and cost all impact assay selection. Emergency situations may necessitate the ability to perform

several different assays to determine dose which includes electron paramagnetic resonance, dicentric chromosome analysis, gamma-(γ) H2AX foci analysis, micronuclei, lymphocyte depletion, premature chromosome condensation (PCC), time to emesis following exposure, and gene expression (Sullivan et al. 2013).

There is a distinction between the Pelger-Huët Anomaly (PHA) and the pseudo Pelger-Huët anomaly (PPHA); PHAs are naturally occurring while PPHAs are induced morphologies. PHAs were first described in 1928 by the German physician, Karl Pelger, and were believed to be a sign of poor prognosis for tuberculosis (Pelger 1928). However, in 1932 G.J Huët discovered PHAs were linked to an autosomal dominant mutation on the long arm of chromosome 1 (Huët 1931). The mutation was in a gene that encodes for the lamin-B receptor, which is a membrane-associated protein embedded in the inner nuclear membrane of the nuclear envelope. The lamin-B receptor has two functions that can be described by its location on the protein. The carboxyl terminus performs C14 sterol reductase activity which involves the breaking of carbon double bonds in cholesterol synthesis, while the amine terminus of the lamin-B receptor binds to an intermediate filament called lamin-B. Lamin-B in turn binds to the chromatin and provides structure to both the chromatin and the nucleoplasm (Holmer et al. 1998). The structure of the nucleus is incredibly important to granulocytes because a hyper-segmented nucleus makes it much easier for these cells to exit the blood vascular compartment via diapedesis. The structure of the nucleus also allows for ease in movement throughout tissues as the cell is migrating to areas undergoing the inflammation response (Colella and Hollensead 2012). An image of the lamin-B receptor with the sterol reductase carboxyl terminus and the chromatin tethering amino terminus can be seen in Figure 1.

While the Pelger-Huët anomaly and pseudo Pelger-Huët anomalies can be seen in any granulocyte, PPHAs are only quantified in neutrophils because they are the most abundant leukocyte in peripheral blood. If the cell morphology is induced from an outside stimulus, such as an exposure to a toxin or ionizing radiation the cells are *pseudo* Pelger-Huët anomalies (PPHAs). PPHAs are distinguishable from other neutrophils in a peripheral blood smear by two factors. The nucleus of the PPHA is bilobular with two lobes that can take on several different shapes and sizes, and the two segments are connected by a very thin nuclear bridge (Goans et al. 2015). While many of the images of PPHAs display a perfectly round to bean-like structure of the two lobes, many of them present with an obscure shape that can be somewhat misleading to the evaluator. Several examples of PPHAs with thin bridges can be seen in Figure 2. A PPHA with an obscure shape to its two lobes and the most common morphology for a neutrophil can be seen in Figure 3.

Some confusion can be experienced when differentiating PPHAs and immature neutrophils. Immature neutrophils remain in the bone marrow through interactions with the chemokine CXCL12 and its receptor CSCR4 (Vietinghoff and Ley 2008). Immature neutrophils are rarely found in the peripheral blood but can escape the bone marrow during an inflammation response. Immature neutrophils in peripheral blood have a band-like morphology as opposed to a multilobed nucleus. In addition, if immature neutrophils enter the peripheral blood in a hypo-segmented form they can be differentiated from PPHAs by the presence of Dohle bodies, fragments of the cells endoplasmic reticulum lost in development. It is likely that

progenitor cells giving rise to granulocytes are impacted by radiation dose to produce the PPHA morphology. Progenitor cells are not terminally differentiated and therefore are more radiosensitive than the postmitotic neutrophils. In addition, other granulocytes (basophils and eosinophils) often present with a bilobed morphology indicating that a common cellular ancestor is being impacted by radiation exposure. As previously stated, basophils and eosinophils are far less common in the peripheral blood under normal physiological conditions, so basophils and eosinophils are not informative biomarkers of radiation dose.

Rhesus macaques (*Macaca mulatta*) were utilized in this study. These animals have an immense population in the wild that results in them being listed as 'least concern' for their conservation status (Singh et al. 2020). Macaque blood physiology is identical to humans (Yu et al. 2019).

The pseudo Pelger-Huët anomalies (PPHA) assay is performed by taking a peripheral blood smear that has been stained with a nuclear staining dye such as Wright-Giemsa stain and evaluated using a light microscope to determine the percentage of neutrophils presenting the PPHA morphology. Previous research projects have shown promising results for chronic exposure from environmental sources, and preliminary data have been produced for acute exposure scenarios, but many questions have been left unanswered (Goans et al. 2015). Biological samples from acutely exposed rhesus macaques were obtained to expand on the previously discovered evidence for the efficacy of the PPHA assay as a biomarker of radiation. This study hypothesized that the PPHA assay will produce a statistically significant dose-response model and will have some degree of persistence following an irradiation incident.

Goans et al. found that humans have a background prevalence of PPHAs of 4.4 ± 0.4%, and rhesus macaques were assumed to have a similar background prevalence. Background radiation is an important consideration for both the baseline and the persistence of PPHAs, as PPHA morphology may be induced by chronic low-dose exposure. The baseline prevalence of PPHAs in rhesus macaques was hypothesized to be above zero, but below the baseline of humans due to primates being irradiated at 5.2 ± 1.3 years of age, while humans were of working ages with higher lifetime doses from background radiation.

Goans et al. conducted a retrospective dose-response study on 8 humans exposed to a mixed field of gamma rays and neutrons during the criticality accident at the Y-12 uranium enrichment facility in 1958 (Goans et al. 2017). A dose-response curve was constructed, however, there was a small sample size, doses were estimated with dose reconstruction models lending to possible error, and the distribution of doses was split into a low dose cohort and a high dose cohort versus a spectrum. The limitations of the Goans et al. study were mitigated here by using well-characterized radiation doses to non-human primates, accumulating a large sample size, and seeking a spectrum of doses for a more robust dose-response curve.

Goans et al. irradiated non-human primates at the Armed Forces Radiobiology Research Institute (AFRRI 2010) using a Co-60 source, and blood smears were taken to investigate how quickly the PPHA morphology began to rise in prevalence within the blood (Goans

et al. 2015). Goans et al documented an increased frequency of PPHAs within 5 hours post-exposure, but a peak prevalence was not documented and whether the prevalence persisted at that peak was not investigated. Persistence was retrospectively investigated by Goans et al. using the survivors of the Y-12 criticality accident, however, with a variety of doses received by the victims of the accident each persistence model only has $n = 1$.

Four specific aims were addressed in this study: (1) Establish baseline prevalence of PPHAs in the peripheral blood of rhesus macaques, (2) establish a dose-response curve across a variety of acute doses, (3) establish a biokinetics and persistence model, (4) determine future study needs to utilize the PPHA assay for biodosimetry.

Methodology

This study was approved by the IACUC of Colorado State University on December 20, 2019 with a Colorado State University IACUC Inter-Institutional Agreement with the Wake Forest School of Medicine, Department of Pathology, Section on Comparative Medicine (WFSM CM). WFSM CM is home to the NHP Radiation Late Effects Cohort. Animal handling, care, and samples being provided by WFSM CM were under the IACUC of the providing institution. WFSM is accredited by the Association for the Assessment and Accreditation of Laboratory Animal Care, International (AAALAC). All procedures involving animals were conducted in accordance with the Animal Welfare Act, and all animals were given environmental enrichment (treats, manipulanda, and social interactions). Safe handling and occupational hazards associated with non-human primates were addressed.

Three distinct PPHA studies were conducted using the blood smears: a baseline prevalence of the PPHA morphology in non-irradiated macaques, a dose-response curve, and a biokinetics/persistence study. Blood smears used in the study were selected from an archive of samples that had been taken as part of periodic wellness testing on the primates at the center. Samples were stained and archived at the time that they were taken, and undisturbed until the time of this project. There were two distinct cohorts of animals that the smears were drawn from, a prospective cohort (PC) and a long-term cohort (LTC). The PC included animals exposed to 4 Gy total body irradiation (TBI), while the LTC was the repository of other radiation-exposed rhesus macaques that were living at the facility, and their blood smears were taken during annual health checkups. All evaluated macaques from both cohorts were used for the dose-response model. The 4 Gy macaques from the PC were used for the biokinetics/persistence model, and all macaques that received 0 Gy of dose, regardless of which cohort they were a part of, were used in the calculation of the baseline prevalence. A table of all macaques, the doses they received, the cohort from which they were drawn, and of which studies they were a part of can be seen in Table 1.

The baseline prevalence of the PPHA morphology was determined by evaluating 18 macaques that were non-irradiated. Six of the PC cohort were non-irradiated, while the 10 that were irradiated contributed blood smears from prior to their irradiation date. In total, 16 macaques contributed blood smears from the PC, and 2 additional macaques that were non-irradiated were taken from the LTC. All values generated were averaged and a standard deviation was calculated.

For the dose-response study, samples were chosen based on an arbitrary time frame of approximately 200 days post-irradiation. The decision to have a narrow time frame was made because the persistence of the PPHA morphology was unknown at the time of selection, so all smears needed to be in the same stage of persistence, or lack of persistence. The selection of the 200-day time frame was simply the availability of macaques with a spectrum of doses from which blood smears had been taken. Of the PC cohort samples, ten blood smears were the pre-irradiation samples, and ten blood smears were approximately 200 days post-irradiation. Samples taken from the PC were not added to the dose-response until after the completion of the biokinetics/persistence study since it was blinded, and time post-irradiation was unknown to the evaluators.

For the biokinetics/persistence study, blood smears were taken from Wake Forest's PC. The cohort consisted of 10 non-irradiated macaques and 10 macaques that were irradiated in October 2016 with a 4 Gy dose. Four of the 10 non-irradiated macaques had succumbed due to comorbidities and were excluded from this study. The remaining 16 macaques (10 irradiated and 6 non-irradiated), all had blood smears taken periodically from 6 days prior to irradiation to 1124 days post-irradiation totaling 19-time points over 3 years and 1 month. Samples were taken on a biweekly basis for the first 2 months, but to minimize the effects of anesthetizing agents on the health of the animal the time frame between smears was spread out to as far as 6 months by the conclusion of the study. The irradiated animals were fixed into 2 groups that were separated merely by the irradiation date. Group information can be seen in Table 1.

Samples from multiple animals were obtained from the WFSM CM NHP Radiation Late Effects Cohort collection for the dose-response study. Irradiated animals received 0 to 8.5 Gy total body radiation using one of two strategies: (1) linear accelerator-produced 6 MV photons (nominal mean energy of 2 MeV), delivered at 80 cGy/minute as a split dose with two parallel-opposed fields, one-half the dose per field; or (2) Cobalt 60-produced gamma irradiation delivered simultaneously, bilaterally at 60 cGy/min. All radiation devices were calibrated using consensus protocols, with validation of dose delivered per animal at the time of irradiation (Table 1 and Supplemental data). The doses delivered are potentially lethal: the LD 10/30 for rhesus macaques is ~5.5 Gy, the LD 50/30 is ~6.7 Gy, and the LD 90/30 is 8 Gy (MacVittie et al. 2015). Surviving animals were subsequently transferred to WFSM CM for research for long-term monitoring post-radiation. Irradiation methods, supportive care strategies, and acute effects for many animals donated to this cohort have been recently reported (Farese et al. 2012; Yu et al. 2015).

All macaques undergo computed tomography (CT) scans as a part of wellness checkups. Animals in the LTC received CT scans upon arrival at WFSM CM, and annually thereafter. PC animals received CT scans in May 2016, April 2018, and March 2020. Three CT scanners were used on animals in this study, Toshiba (2012–2017), GE (2018), and Siemens (2019-present). The Toshiba delivered an average dose of 35.7 mSv/yr (or 0.036 Gy/yr), the GE delivered an average dose of 39.2 mSv/yr (or 0.039 Gy/yr), and the new Siemens delivers an average dose of 18 mSv/yr (or 0.018 Gy/yr). The dose received from the CT was inconsequential compared to the animal's acute doses and so was not considered a significant factor in PPHA frequency.

Peripheral blood slides were prepared by laboratory technicians at WFSM CM on the day of the blood sampling, or necropsy for deceased cohorts. All blood smears were fixed with methanol, air dried, stained using Wright-Giemsa stain, and subsequently, air-dried again. Blood smears were manually inspected under an Olympus BH-2 light microscope at 400x magnification. The slide was placed on the stage and low viscosity Thermo Scientific Resolve™ microscope immersion oil was used to maximize clarity of evaluation. The slide was first quickly inspected for clarity of staining, quality of cells, and ultimately the ability to continue with the PPHA analysis. Once the slide was determined to be suitable, neutrophils were counted in a sweeping back and forth raster scan that was systematic in nature to ensure that cells were not counted more than once. A count of neutrophils was kept until a PPHA was encountered. At that time, the number of neutrophils counted, including the PPHA, was recorded in a laboratory notebook. The microscope magnification was then increased to 1000x using oil immersion for closer inspection of the suspect PPHA. If it was determined to be a PPHA, an image was taken using a 12-megapixel Galaxy S8+ smartphone with a Gosky microscope lens smartphone camera adapter, and the PPHA was recorded in the laboratory notebook as a hashmark on a different line below the neutrophil count. This process was continued until the cumulative count of neutrophils, including PPHAs, reached 300 cells. This process was repeated for every blood smear evaluated. Following evaluation, evaluations were reconciled with the sample identification number and recorded on a spreadsheet for later analysis.

When evaluating blood smears manually there is an inherent risk of bias by the evaluator for considering neutrophils to be PPHAs when they are ultimately not. Several steps were taken to mitigate this risk of bias in the analysis and the data produced. For the dose-response study, animal IDs were known by the evaluator at the time of evaluation, but radiation doses were blinded until after the last animal was evaluated. For the biokinetics and persistence study, since all animals had the same dose, the only means of preventing bias was to blind the dates the animals were evaluated and include several 0 Gy macaques. The PC contained 10 macaques that received 4 Gy, 6 macaques that received 0 Gy, and 1000 blood smears across 10 slide boxes. The boxes of blood smears were labeled with the window of time that corresponded to the blood smears they contained. A piece of tape was placed over these labels and the boxes were randomly placed out of order. In addition, when slides were evaluated the following day, a small piece of tape was placed over the date on the label on the slide itself. Lastly, an image was taken of every PPHA found. All images were reconciled and labeled with the associated macaque the day after evaluation at the same time the data and slides were reconciled and added to the spreadsheet. Images were inspected using a large computer monitor to allow for the evaluation of the cell’s morphology. At the conclusion of every week, all images were reviewed once again, data on the spreadsheet were checked against the laboratory notebook, and microscope slides were returned to the appropriate box and placed in a complete stack. All cells that were erroneously determined as PPHAs were annotated in the laboratory notebook and the digital spreadsheet. Timestamp labels on the slide boxes were not removed until all 10 slide boxes were placed in the complete pile.

For each sample, the number of PPHAs observed in a blood smear was compared to the total number of neutrophils counted to determine a percentage of cells with the PPHA

morphology. Percentages were aligned with the doses and plotted to evaluate dose-response relationships. Regression analysis was performed on the dose-response using Microsoft Excel to determine correlation coefficients and statistical significance of the data. Since the dose-response had multiple animals clustered at 0, 4, 6.4–6.5, and 8–8.5 Gy, box and whisker plots were also constructed to display the distribution of data within the cohorts. A Shapiro-Wilk test was performed to test for the normality of the data. Subsequently, nonparametric comparisons for each dose group using the Wilcoxon method without the assumption of normality were performed to look for statistically significant differences.

Results

The baseline prevalence of the PPHA morphology in the rhesus macaques was determined to be 0.58 ± 0.46% with a lower limit of 0% and an upper limit of 1%. Baseline prevalence data took on a normal distribution that was insignificantly skewed positively. Because the skew factor was not significant, data were analyzed without log transformation. The distribution of baseline percentages of PPHAs can be seen in Figure 4, and the Macaque identification numbers with the individual percentage of neutrophils presenting with the PPHA morphology can be seen in Table 2.

A linear dose-response relationship was found between the percentage of neutrophils that presented the PPHA morphology and the acute radiation dose administered to the rhesus macaques (Figure 5). The linear trendline displayed a positive correlation between PPHAs and radiation dose with an R^2 of 0.88 with a standard error of 0.53 ($p = 3.62 \times 10^{-22}$). Blood smears for the dose-response were taken from the animals at an average of 198 ± 8.2 days following irradiation including the macaques used from the biokinetics/persistence study. Data points in the dose-response graph are displayed as semi-translucent so that data points with multiple animals appear darker. Each animal had only one blood smear available for analysis, so no animal average or standard deviation is reported. The dose-response model and corresponding linear regression line can be seen in Figure 5. Dose-response samples were clustered at 0, 4, 6.4–6.5, and 8–8.5 Gy. The number of animals and distribution of data can be seen in Table 2.

A Shapiro-Wilk test showed that the data was not normally distributed ($p = .0365$). This was not surprising since the bottom end of the distribution is not zero, even in unirradiated animals. A nonparametric comparison for each cohort using the Wilcoxon method not assuming normality was performed. The 0 Gy and 4 Gy cohorts were statistically different at the 95% confidence level, with a p-value of 4.75×10^{-7}, the 4 Gy cohort and the 6.4–6.5 Gy cohort were statistically different at the 95% confidence level, with a p-value of 2.18×10^{-3}, and the 6.4–6.5 Gy cohort and the 8–8.5 Gy cohort was statistically different at the 95% confidence level, with a p-value of 2.02×10^{-2} (Figure 6).

The standard deviation of each cohort was expected to increase with increasing radiation dose due to the inherently random nature of damage due to ionizing radiation. In addition, cellular repair mechanisms respond at different rates in different individuals lending to increased variance of outcomes. The standard deviation only increased minimally with increasing dose.

The 10 animals in the biokinetics/persistence study were evaluated for PPHAs prior to irradiation, and post-irradiation. Rhesus macaques acted as their own controls in this experiment, and the average baseline percentage of PPHAs used for comparison with post-irradiation PPHA percentages was calculated using only the 10 rhesus macaques irradiated with 4 Gy in the PC. The 8 additional animals that received 0 Gy of irradiation were not factored into the baseline average for the biokinetics/persistence study. The average baseline percentage of PPHAs for control samples was 0.73 ± 0.58%. The baseline average of the biokinetics/persistence study (0.73 ± 0.58%) was compared to the average of the full baselines study (0.58 ± 0.46%) using a Students t-test and there was not a statistically significant difference between them ($p = .38$). The earliest time point following irradiation that was available for analysis was 24–48 hours post-irradiation. The average prevalence of the PPHA morphology 24–48 hours post-irradiation was 1.94 ± 1.03%, which is an increase of 233% from pre-irradiation. The next data point was 1.2 weeks post-irradiation, and the average prevalence of the PPHA morphology was 2.80 ± 0.60%, which is an increase of 350% from the baseline. Following one week post-irradiation, the prevalence plateaued and was relatively constant. The increase in the prevalence of the PPHA morphology and up to 4 weeks post-irradiation can be seen in Figure 7.

The last time point evaluated for each macaque had an average increased prevalence of PPHAs of 2.7 ± 0.28% which is a 338% increase from the pre-irradiation average PPHA prevalence of 0.73 ± 0.58%. When the average of the last time point is compared with the average of 1.2 weeks post-irradiation (when the prevalence plateaued) a change of only −0.1% PPHA prevalence is observed over 3 years. The change in prevalence from 1.2 weeks post-irradiation to 3.1 years post-irradiation is less than one standard deviation, indicating a negligible change in the prevalence and persistence of the PPHA morphology to 3 years post-irradiation. Furthermore, an average was taken of all PPHA evaluations across all animals in the study from the start of the prevalence plateau (1.2 weeks post-irradiation) through the end of the study (3.1 years post-irradiation), and the average PPHA percentage was 2.7 ± 0.33% which is a 338% increase from the pre-irradiation average. An overlay of the 10 independent biokinetics curves can be seen in Figure 8, an average of the 10 animals can be seen in Figure 9, and data associated with the average of all 10 animals can be seen in Table 3.

Discussion

The baseline prevalence of the PPHA morphology in rhesus macaques was found to be 0.58 ± 0.46% ($n = 18$). Goans et al. reported a background percentage of PPHAs in humans to be 4.4 ± 0.4% ($n = 16$) (Goans et al. 2017). A baseline prevalence of PPHAs is indicative that there are other causes for the PPHA morphology to be present in the peripheral blood besides an acute radiation dose. A probable cause of the baseline prevalence is age-related and due to the accumulation of radiation dose from background radiation sources. Rhesus Macaques have a life expectancy of approximately 25 years and the average age of the zero Gy dose animals when blood smears were taken was 5.2 ± 1.3 years old. The average age of the humans in the control group was not reported (Goans et al. 2017) but was given as equivalent to the exposed radiation workers in the retrospective study of the Y-12 criticality accident. The humans investigated for baseline prevalence were much older than the rhesus

macaques studied, and this is a possible explanation for the much higher background prevalence of PPHAs in humans than in the macaques. The change in baseline prevalence of PPHAs as an organism ages warrants further investigation into how background radiation impacts the baseline prevalence, and correction factors for age will be necessary.

The dose-response study found a positive correlation between the percentage of neutrophils present in the peripheral blood with a PPHA morphology and acute radiation dose. A linear trendline of PPHA cells and radiation dose yielded an *R*-squared of 0.88. The blood smears available to use were all archived samples, and since the biokinetics was unknown for the PPHA morphology following an acute radiation dose, the spectrum of radiation doses was limited to those available in a small window of time following the irradiation event. The largest spread of doses inside the narrowest available timeframe included 6 dose cohorts (0, 4, 6.4, 6.5, 8, and 8.5 Gy) that were taken at 198 ± 8 days post-irradiation. The 6.4, 8, and 8.5 Gy cohorts only contained 4 rhesus macaques total, so they are a part of the dose-response model (Figure 5) but were removed from the box and whiskers plot (Figure 6). A Students *t*-test confirmed a statistically significant difference between the 0 and 4 Gy cohorts, and the 4 and 6.5 Gy cohorts.

Detection limits and minimum dose for response could not be determined in this study. A statistical difference between the baseline macaques and the 4 Gy macaques was found, but there were no animals sampled between 0 and 4 Gy due to a lack of availability in the window of time chosen. With the results of the biokinetics study showing that the maximum prevalence of the PPHAs was reached in 1.2 weeks and persistence was observed after that, future samples can be analyzed and added to the dose-response outside of the 198 ± 8-day windows to fill the gaps between the dose cohorts. Additionally, LD 50/30 for rhesus macaques is reported to be 6.7 Gy, while LD 50/30 for humans is 3.5 Gy (MacVittie et al. 2015). A lower LD 50/30 in humans demonstrates the need for the determination of lower limits of detection so that decisions can be made during the triage phase following a mass casualty incident.

The rapid increase of the PPHA morphology indicates that it can be used for quick estimation of dose, and persistence to 3 years demonstrates that it can be used for retrospective dose estimation as well. However, only two blood smears were taken between irradiation and the peak PPHA percentage being reached, 1 day and 8 days post-irradiation (Figure 7). On the first day, nearly a 3-fold increase of PPHAs was reported going from a baseline of 0.7–1.9%. In the next week, the PPHA percentage increased further to a 4-fold increase of 2.8% (Table 3). To characterize the rise in prevalence of the PPHA morphology more accurately, blood smears need to be taken at regular intervals until the reported values plateau. The estimated blood sampling interval for PPHA in future studies should be approximately 5 hours, based on Goans et al. reporting a rise in PPHA quantities in as little as 5 hours. Methods of extracting blood from the animal will need to be determined with the well-being of the animal's health in mind. The frequent handling and extraction of biological samples can cause a significant amount of stress and complications including a higher risk of death.

A trendline was drawn between the irradiation date and one-day post-irradiation ($y = 5.6279x + 0.73$) and when the maximum value of 2.8% PPHAs was entered into the trendline equation, the interpolated time to reach maximum PPHA concentration is estimated to be 62 hours post-irradiation if the rate of increase was constant (Figure 7). A 5-hour interval of sampling would result in 13-time points until the plateau is reached. Unfortunately, additional sampling was not possible as this was a retrospective study, and future research would require different animals. However, the 10 macaques in the biokinetics study are still alive with samples being taken periodically, so the persistence models can be extended from 3.1 years to 4 years post-irradiation as of December 2020 (Figures 8 and 9).

PPHAs present themselves in granulocytes versus T-lymphocytes which are the subject of dicentric chromosome assays, and granulocytes have an average lifespan in the blood of around 8 hours (Ramalho et al. 1995). PPHAs have persisted in rhesus macaques for 3 years despite the extremely short lifespan of neutrophils because the cells suspected of being affected by radiation are progenitor cells and hematopoietic stems cells in the bone marrow. The exact mechanism that causes the formation of PPHAs is unknown, but there are two possibilities for PPHA proliferations. First, a mutation in chromosome one impacts translation of the lamin-b receptor and degrades the integrity of the nuclear membrane. Second, physical interaction of radiation with chromatin causes a bridge to be formed and the cell is unable to complete cytokinesis or unable to fully segment.

The presence of the PPHA morphology in peripheral blood smears may be useful as an inexpensive and effective biomarker of acute radiation exposure. However, the relationship between the percentages of neutrophils that display the PPHA morphology and acute radiation dose needs strengthening to ensure confidence in the macaque models and translation to humans in a mass casualty incident. The dose-response is limited by the small number of cohorts that were available for evaluation. The biokinetics study was limited because blood smears were taken at only two-time points in the first week following irradiation. Lastly, the persistence model was only evaluated to 3.1 years and a point where the peripheral prevalence of PPHAs begins to drop was not found.

We recognize that our findings are not generated from human subjects. In the case of isolated human exposures, individual patient symptoms will likely be more relevant than a single measurement of PPHA. The real value of the PPHA approach will be in the event of large-scale exposures. Adaptation of the PPHA assay to prevailing human baselines will be necessary at that time since PPHAs can reasonably be expected to vary by geographic location and other factors even among human subjects.

Future directions for this work might include the comparison to assays such as the dicentric chromosome assay in parallel to validate the PPHA assay as a biomarker of acute radiation dose. Secondly, the differentiation of the PPHA from normal neutrophils is conducted purely from visual inspection, which could be subjective. While images were taken to verify the decisions, molecular characterization and the origin of the PPHA morphology could make determining what is a PPHA and what is a normal neutrophil far more consistent. However, the doses in this study were known quite precisely, and the most relevant comparison is not to another surrogate biomarker, but to the known dose given.

Conclusions

This study was intended to expand upon the methodologies available to biodosimetrists for early and retrospective radiation dose estimations for individuals that have been exposed to acute doses of ionizing radiation. While the models built for this project are more robust than previous studies, shortcomings are present. The dose-response model has dose cohorts versus a spectrum, the first-week post-irradiation needs to be characterized further, and the persistence was not observed past 3.1 years so a time-related reduction of the PPHA morphology in peripheral blood was not found. Future projects will include analysis of more zero dose rhesus macaques to increase confidence in baseline, an expansion of the dose-response model by adding additional animals to increase a variety of doses, extending the biokinetics model beyond the available 3.1 years of blood smears, and increasing frequency of blood smears taken immediately the following irradiation to better characterize the initial peak of PPHA prevalence. Additional anticipated areas of research needed are to molecularly characterize the PPHA morphology, seek to validate the PPHA assay with dicentric chromosome analysis in a paired study, and investigating the efficacy of PPHA assay automation using metasystem microscopes that are currently in use for dicentric chromosome analysis.

Many biodosimetry assays have immense logistical requirements which highlight the need for methods that are low cost, quick, and accurate. The PPHA assay demonstrates the potential to fill these needs. It can be low cost because the necessary equipment includes glass slides, a nuclear stain, coverslips, and a light microscope; all of which are common laboratory equipment. It can be quick because the microscope slide only takes a trained technician less than 15 minutes to evaluate, and in fact, the longest portion of the assay is fixing and staining the blood sample on the slide. Lastly, the PPHA assay can also be accurate if the exact mechanism of origin is discovered and a system of repeated laboratory irradiation and evaluation of samples can occur to narrow down detection limits, much like what has been done with dicentric chromosome analysis.

Supplementary Material

Refer to Web version on PubMed Central for supplementary material.

Funding

This work was supported by the grant T42OH009229, funded by the National Institute of Occupational Safety and Health in the Centers for Disease Control and Prevention. Its contents are solely the responsibility of the authors and do not necessarily represent the official views of the Centers for Disease Control and Prevention or the Department of Health and Human Services. This work was additionally supported in part by NIH U01AI150578 (JM Cline, PI), NIH U19A167798 (N Chao, PI) and DOD CDMRP W81XWH-15-1-0574 (JM Cline, PI).

References

Armed Forces Radiobiology Research Institute [AFRRI]. 2010. Medical management of radiological casualty’s handbook. Bethesda (MD); 2010. Online 3rd Edition.

Colella R, Hollensead SC. 2012. Understanding and recognizing the Pelger-Huet anomaly. Am J Clin Pathol. 137(3):358–366. [PubMed: 22338047]

Farese AM, Cohen MV, Katz BP, Smith CP, Jackson W, Cohen DM 3rd, MacVittie TJ. 2012. A nonhuman primate model of the hematopoietic acute radiation syndrome plus medical management. Health Phys. 103(4):367–382. [PubMed: 22929469]

Goans RE, Iddins CJ, Christensen D, Wiley A, Dainiak N. 2015. Appearance of pseudo-Pelger Huet anomaly after accidental exposure to ionizing radiation in vivo. Health Phys. 108(3):303–307. [PubMed: 25627941]

Goans RE, Iddins CJ, Ossetrova NI, Ney PH, Dainiak N. 2017. The pseudo-Pelger Huët cell-a new permanent radiation biomarker. Health Phys. 112(3):252–257. [PubMed: 28121725]

Hayes J 2018. The pseudo Pelger-Huët anomoly as a potential biomarker for chronic low-dose radiation exposures ff sus scrofa leucomystax and apodemus speciosus [master's thesis]. Fort Collins (CO): Colorado State University.

Holmer L, Pezhman A, Worman HJ. 1998. The human lamin B receptor/sterol reductase multigene family. Genomics. 54(3):469–476. [PubMed: 9878250]

Huët GJ. 1931. Familial anomaly of leukocytes. Nederl Tijdschr Genneesk. 75:5956–5959.

MacVittie TJ, Farese AM, Jackson W 3rd 2015. The hematopoietic syndrome of the acute radiation syndrome in rhesus macaques: a systematic review of the lethal dose response relationship. Health Phys. 109(5):342–366. [PubMed: 26425897]

Pelger K 1928. Demonstrate van een paar zeldzaamvoorkomend de typen van bloedlichaapjes en bespreking der patienten n. Nederl Tijdschr Geneesk. 72:1178.

Ramalho A, Curado M, Natarajan A. 1995. Lifespan of human lymphocytes estimated during a six-year cytogenetic follow-up of individuals accidentally exposed in the 1987 radiological accident in Brazil. Mutat Res Fundam Mol Mech Mutagen. 331(1):47–54.

Singh M, Kumar A, Kumara HN. 2020. "Macaca mulatta". IUCN Red List of Threatened Species. 2020: e.T12554A17950825.

Sullivan JM, Prasanna PG, Grace MB, Wathen LK, Wallace RL, Koerner JF, Coleman CN. 2013. Assessment of biodosimetry methods for a mass-casualty radiological incident: medical response and management considerations. Health Phys. 105(6):540–554. [PubMed: 24162058]

Vietinghoff S, Ley K. 2008. Homeostatic regulation of blood neutrophil counts. J Immunol Res. 181(8):5183–5188.

Yu JZ, Lindeblad M, Lyubimov A, Neri F, Smith B, Szilagyi E, Halliday L, MacVittie T, Nanda J, Bartholomew A. 2015. Subject-based versus population-based care after radiation exposure. Radiat Res. 184(1): 46–55. [PubMed: 26121229]

Yu W, Hao X, Yang F, Ma J, Zhao Y, Li Y, Wang J, Xu H, Chen L, Liu Q, et al. 2019. Hematological and biochemical parameters for Chinese rhesus macaque. PLoS One. 14(9):e0222338. [PubMed: 31527891]

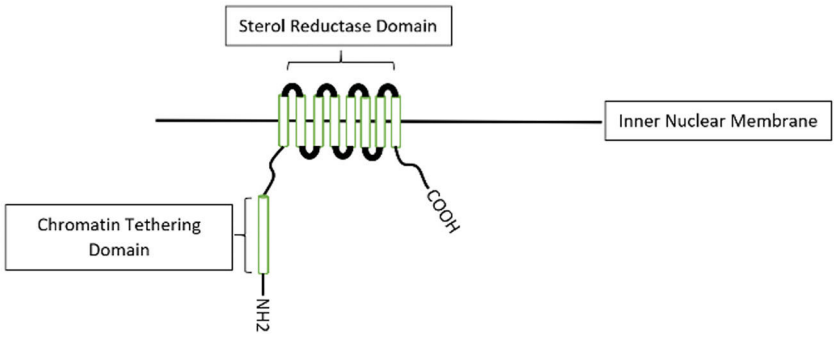

Figure 1.
Structure of the lamin-B receptor (Hayes 2018).

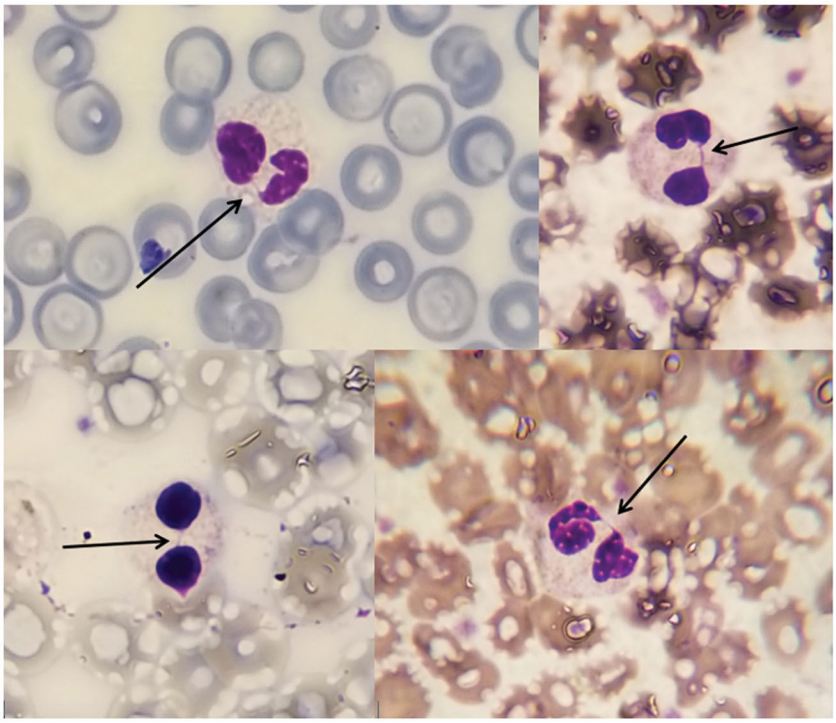

Figure 2.
Examples of pseudo Pelger-Huët anomalies, and their various shapes of the two lobes. The thin bridge connecting the two lobes can be seen in each image (black arrow).

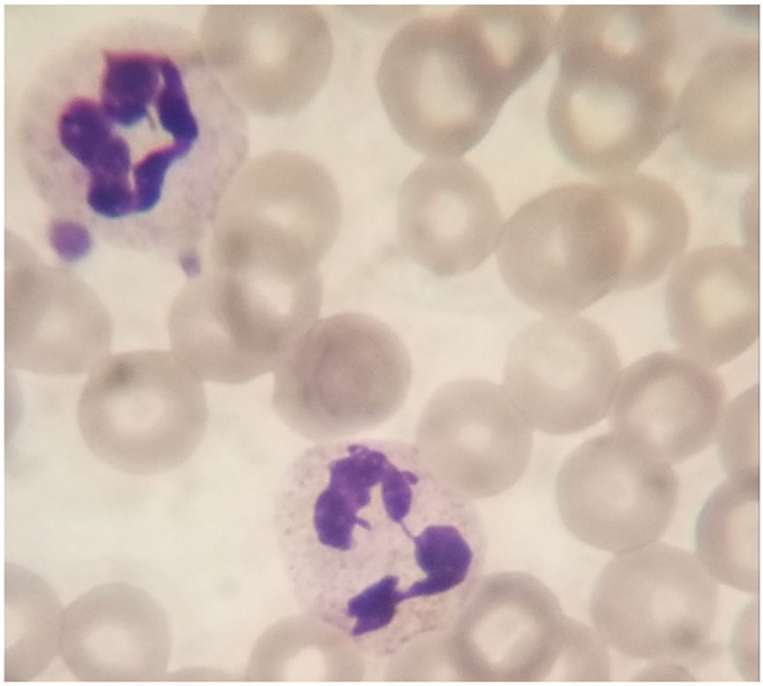

Figure 3.
Example of a normal neutrophil (A), next to a Pseudo Pelger-Huët anomaly (B), from macaque 1905, blood smear taken on November 24, 2015.

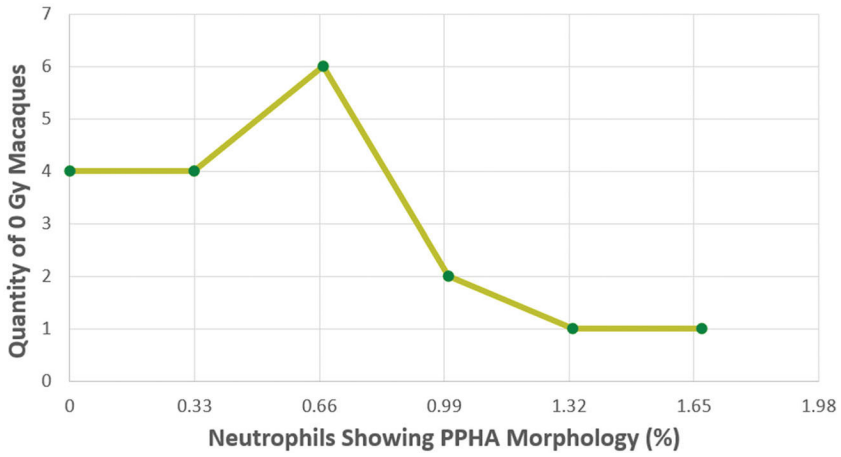

Figure 4.

Distribution of the percentage of neutrophils presenting with PPHA morphology in 0 Gy dose rhesus macaques.

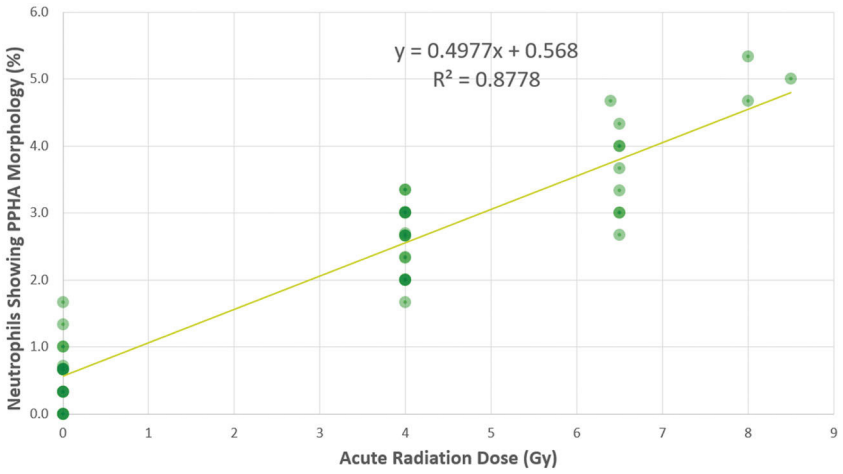

Figure 5.

Rhesus macaque dose-response displaying a linear relationship between the percentage of neutrophils presenting the PPHA morphology and acute radiation dose.

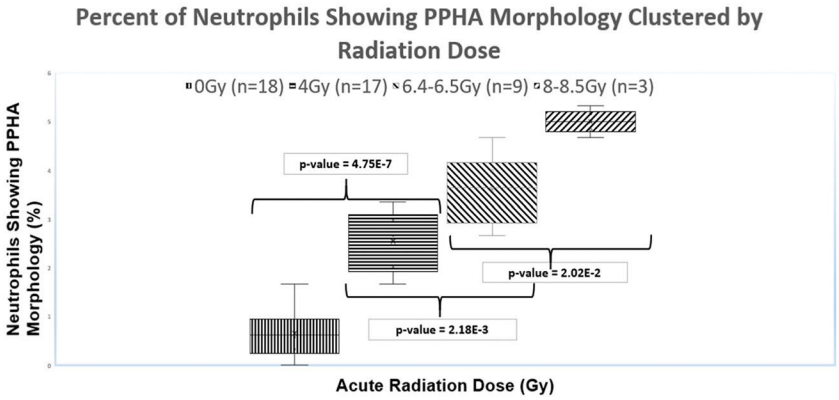

Figure 6.

Rhesus macaque dose-response with animals clustered by dose (0 Gy, 4 Gy, 6.4–6.5 Gy, and 8–8.5 Gy). The upper and lower limits of recorded values are denoted with the upper and lower whiskers on each plot.

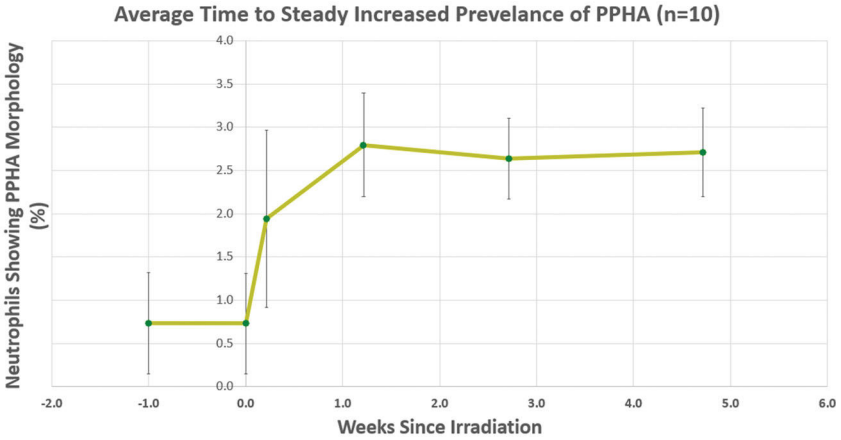

Figure 7.

Rhesus macaque average time to a steady increase in the prevalence of pseudo Pelger-Huët anomalies as a function of weeks post-irradiation.

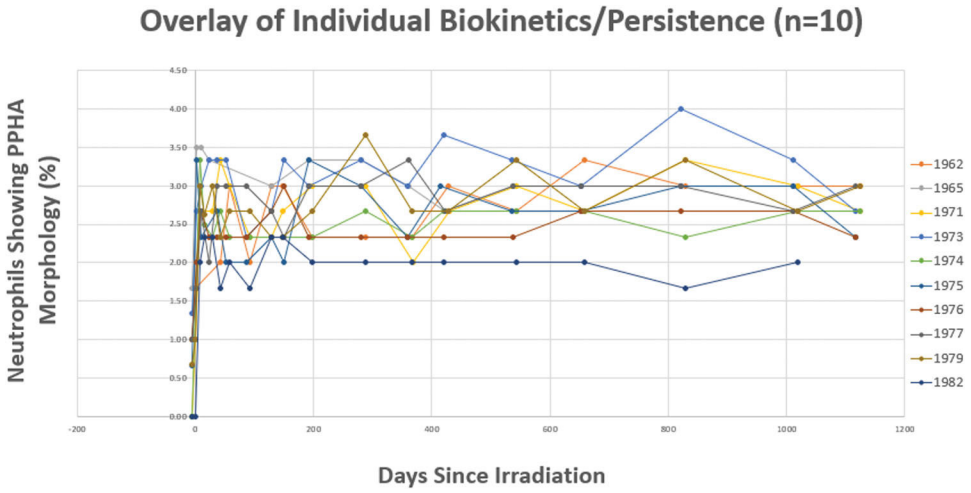

Figure 8.
Rhesus macaque biokinetics/persistence with 10 subject animals overlayed.

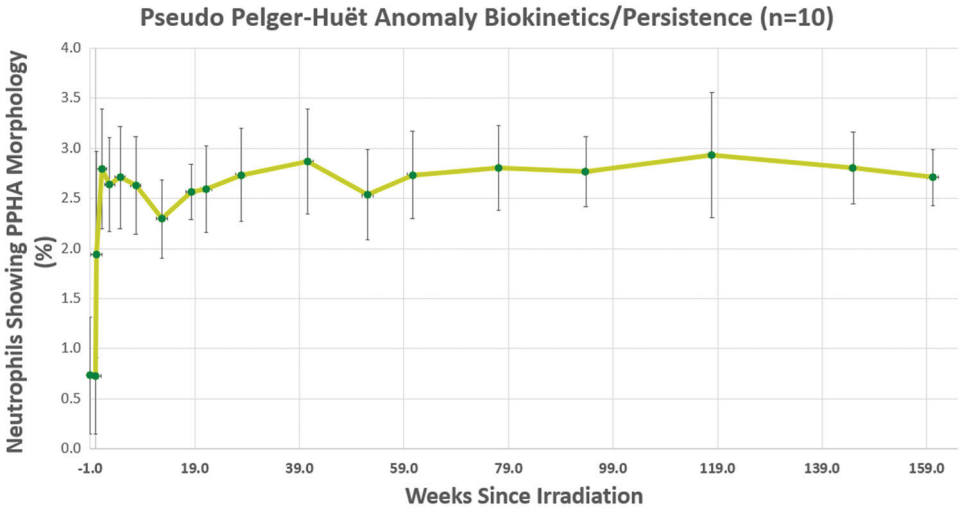

Figure 9.

Rhesus macaque biokinetics/persistence, average PPHA concentration by weeks post-irradiation.

Table 1.

Dose and study enrollment of animals.

Animal *N*	Cohort	Dose (Gy)	Radiation source	Dose rate (Gy/min)	Dosimetry device	Baseline Unirradiated	Dose-response	Biokinetics/Persistence
2	LEC	0	Co60 sham	0	IC	✓	✓	✗
10	PC	0, 4	LINAC	0.8	IC	✓	✓	✓
6	PC	0, 4	Co60	0.6	IC + ND	✓	✓	✓
1	LEC	4	LINAC	0.7	DD	✗	✓	✗
6	LEC	4	Co60	0.6	IC	✗	✓	✗
9	LEC	6.4–6.5	LINAC	0.8	IC	✗	✓	✗
3	LEC	8–8.5	LINAC	0.8	IC	✗	✓	✗

LEC: late effects cohort; PC: prospective cohort; IC: ionization chamber; ND: nanodot; DD: diode detector.

Table 2.

Averages of 0, 4, 6.4–6.5, and 8–8.5 Gy rhesus macaques.

	n	Average PPHA (%)
0Gy	18	0.58 ± 0.46%
4 Gy	17	2.57 ± 0.51%
6.4–6.5 Gy	9	3.50 ±0.59%
8–8.5 Gy	3	5.00 ± 0.59%

Table 3.

Rhesus macaque biokinetics/persistence with n-10 averaged at weeks post-irradiation.

Average biokinetics/persistence group 1&2 (n = 10)		
Weeks post-irradiation	**Average PPHA (*n* = 10)**	**Std. Dev. (±)**
−1.00	0.73	0.58
0.00	0.73	0.58
0.22	1.94	1.03
1.22	2.80	0.60
2.72	2.64	0.47
4.72	2.71	0.51
7.71	2.63	0.48
12.72	2.30	0.39
18.29	2.57	0.27
21.22	2.59	0.43
27.86	2.73	0.47
40.64	2.87	0.53
52.07	2.53	0.45
60.64	2.73	0.44
77.14	2.80	0.42
93.77	2.77	0.35
117.93	2.93	0.62
144.93	2.80	0.36
160.20	2.71	0.28